IOSR Journal Of Applied Physics (IOSR-JAP)
e-ISSN: 2278-4861.Volume 12, Issue 4 Ser. II (Jul. – Aug 2020), PP 50-57
www.Iosrjournals.Org

Determination of Absorption Coefficients from Q_T and Q_L propagation of signal frequency in Equatorial Ionosphere at Sunset

Ekong U. Nathaniel[1], Samuel T. Ebong[2]
[1,2]Department of Physics, Akwa Ibom State University, Nigeria

Abstract
Absorption coefficients from Q_T and Q_L propagation of signal frequency in equatorial ionosphere at sunset have been investigated. Non-deviative and deviative absorption have been identified with known refractive index. Using sunset data, absorption coefficients decrease as the sunset moves into night indicating that absorption coefficients depend on solar intensity. The relationship between electron density, N and the absorption coefficient, K is less of a logarithmic and more of a moving average.
Keywords: *Absorption, Quasi-Longitudinal (Q_L), Quasi-Transverse (Q_T)*

Date of Submission: 11-08-2020 Date of Acceptance: 27-08-2020

I. Introduction

A signal of 4.9MHz transmitted from Cotonou at latitude 6°22' N, longitude 2°26E with antenna that is horizontally polarized log-periodic with narrow azimuth pattern, received at Lagos at latitude 6°27' N, longitude 3°28' E with antenna that is horizontally linear polarized, half wavelength dipole placed $\frac{\lambda}{4}$ above the ground. The frequency range is 3-20MHz and the take off angle of 45° (Shamsi, 1984, V. Chukwuma, 1999). The data gathered from this propagation has been useful in this work.

At the rather high frequencies that are currently used in trans-ionospheric radio links, the wave path is not much influenced by birefringence in the magnetized plasma. The polarization status of the wave is very sensitive to it. So, the polarization changes must be expected even at quite high frequencies. They are due to the fact that any radio wave entering the magnetized plasma such as the earth ionosphere is decomposed into two characteristic polarizations. When travelling through the ionosphere, the two waves suffer from different phase changes so that they arrive at the upper edge of the ionosphere with clear phase difference. When the principal polarization at the entrance into the ionosphere is almost circular, quasi-longitudinal (Q_L) propagation is considered or rather circular polarization (C_p). But when the principal polarization is linear, quasi-transverse (Q_T) propagation is considered or rather linear polarization (L_p) (Rawer, (1993); Unal, I., et al.(2007)). The radio wave propagation and the absorption have been investigated by various researchers such as Nathaniel, E. U. et al (2020), Unal . I. et al. (2007), and Zabotin N. A. et al. (1997).

Electron density, collision frequency, absorption and absorption coefficients

With any given signal frequency, the maximum electron density can be calculated at the point of reflection of the wave in the ionosphere (Olatunji, E. O. (1966), King, J. W. et al (1967)) . As a condition of reflection of wave in plasma, signal frequency, f must be equal to the plasma frequency, F_N (Rawer, 1993, Kelso, 1956).

$$f = f_N;\ \omega = \omega_N \qquad 1$$

The reduced electron density X according to J.M. Kelso is

$$X = \frac{\omega^2{}_N}{\omega^2} = \frac{f^2{}_N}{f^2} = \frac{Ne^2}{m\varepsilon_0\,\omega^2} \qquad 2$$

X = reduced electron density; e = electron charge = 1.602×10^{-19} C
M = electron mass = 9.11×10^{-31}kg; ε_0= permittivity of free space
$\varepsilon_0 = 8.85 \times 10^{-12}$ H/m ; ω = operating angular frequency
At the point of reflection, X = 1 and the plasma frequency becomes the critical frequency, f_0.
Therefore,

$$N_m = \frac{m\varepsilon_0\omega^2}{e^2} = \frac{4\times9.11\times10^{-31}\times8.85\times10^{-12}\times(3.142)^2\times f_0{}^2}{(1.602\times10^{-19})^2}$$

$= 1.240 \text{ x } 10^{-2} {f_0}^2$ (f_0 is in Hz, N_m is in m^{-3}) 3

From the magneto-ionic theory, most investigators dealt with the propagation of electromagnetic waves in ionized gases and the derivations simplified. Three customary magnetoionic parameters are given as

$$X = \frac{\omega^2{}_N}{\omega^2}; Y = \frac{\omega_G}{\omega}; Z = \frac{\nu}{\omega} \quad 4$$

The basic thing about these parameters is that they are ratios three different quantities to operating angular frequency, ω.

Plasma; $\omega^2{}_N = (2\pi f_N)^2 = \frac{Ne^2}{m\varepsilon_0}$ 5

Gyro (G); $\omega^2{}_G = (2\pi f_G)^2 = \left(\frac{Be}{m}\right)^2$ 6

B = flux density of the earth's magnetic field
υ = collision frequency of electrons with other particles
If θ is the angle between the direction of the wave normal and the magnetic field, then
Y_L = Ycosθ (longitudinal component)
Y_T = Ysinθ (transverse component)
In the presence of the magnetic field, the ionosphere is a doubly refracting medium and the two modes of propagation exist for which the names "ordinary" and extraordinary" are considered (Titheridge, J. E.(1966); Baumjohann, W. et al (1996); Kivelson, M. G. et al. (1995); Parks, G. K.(1991); Folkestad, K. et al (1968).
The ionosphere is a complex medium with a complex refraction index (Rawer 1967)
Refractive index, $n = \mu - i\psi$ 7
μ = real part
ψ = imaginary part

$$n^2 = (\mu - i\psi)^2 = \mu^2 + \psi^2 - 2i\mu\psi \quad 8$$

Following Appleton – Hartree formula for a complex refractive index, n

$$n^2 = 1 - \frac{X}{1 - iZ - \frac{Y^2{}_T}{2(1-iZ-X)} \pm \sqrt{\frac{Y^4{}_T}{4(1-iZ-X)} + Y^2{}_L}} \quad 9$$

According to Rawer,
Q_T propagation approximation is valid for

$$\frac{Y^4{}_T}{4(1-iz-X)} \gg Y^2{}_L \quad 10$$

$$n^2 = 1 - \frac{X}{1-iZ} \quad 11$$

Rationalizing the surd,

$$n^2 = 1 - \frac{X(1+iZ)}{(1-iZ)(1+iZ)} = 1 - \frac{X}{1+Z^2} - \frac{iXZ}{1+Z^2} \quad 12$$

Separating the real and the imaginary parts of the equations $n^2 = \mu^2 + \psi^2 - 2i\mu\psi$; $n^2 = p + q$;
real part = p, q = imaginary part
Real; $p = \mu^2 + \psi^2$, but $\mu^2 \gg \psi^2$ 13
Hence, $p \approx \mu^2 = 1 - \frac{X}{1+Z^2}$ 14

$Z^2 \ll 1$
$p = \mu^2 = 1 - X$ 15
Imaginary: $q = 2\mu\psi = \frac{XZ}{1+Z^2}$

$$\psi = \frac{XZ}{2\mu(1+Z^2)} \quad 16$$

Absorption coefficient K is given by I. Unal et al and E. V. Thrane et al to be the product of the wave number κ and the imaginary part of the wave, ψ.

$$K = \frac{\omega}{c}\psi = \kappa\psi; \kappa = \frac{\omega}{c} \quad 17a$$

$$K_1 = \frac{\omega}{c}\frac{XZ}{2\mu(1+Z^2)} \quad 17b$$

Absorption here is the loss of energy when electrons oscillating under the influence of a radio wave make collisions with other particles (Mishin, E. V et al, 1995, Belova, E. G et al.1995, Nielsen, E., et al, 2007).

Absorption $L_1(dB) = \int K ds = \int \frac{\omega}{c}\psi ds = \frac{\omega}{c}\int \psi ds = \frac{\omega}{2\mu c}\int \frac{XZ}{(1+Z^2)} ds$ 18

This is valid for Q_T propagation

Also, $Y_L{}^2 \gg \frac{Y_T{}^4}{4(1-iZ-X)^2}$ is a condition which Q_L is valid.

$$n^2 = 1 - \frac{X}{1-iZ+Y_L} = 1 - \frac{X((1+Y_L)+iZ)}{(1+Y_L-iZ)(1+Y_L+iZ)}$$

$$n^2 = 1 - \frac{X(1+Y_L)}{(1+Y_L)^2+Z^2} - \frac{iXZ}{(1+Y_L)^2+Z^2}$$

$$(1+Y_L)^2 \gg Z^2$$

Therefore,

$$n^2 = 1 - \frac{X}{(1+Y_L)} - \frac{iXZ}{(1+Y_L)^2} \qquad 19$$

Separating the real and imaginary parts

Real: $p = \mu^2(\mu^2 \gg \psi^2) = 1 - \frac{X}{(1+Y_L)}$ 20

Imaginary: $q = 2\mu\psi = \frac{XZ}{(1+Y_L)^2}$

$$\psi = \frac{XZ}{2\mu(1+Y_L)^2}$$

Absorption coefficient $K_2 = \frac{\omega}{c}\psi$

$$= \frac{\omega XZ}{2\mu c\,(1+Y_L)^2}$$

Absorption $L_2(dB) = \frac{\omega}{c}\int \psi ds$

$$= \frac{\omega}{2\mu c}\int \frac{XZ}{(1+Y_L)^2} ds \qquad 21$$

This is valid for Q_L approximation where the angle between the magnetic field and the direction of wave is very small.

The absorption coefficient depends on

- The mean energy picked up by the electron from the wave
- The number of collisions per unit volume per unit time
- The speed with which the wave traverses the medium

The longitudinal component Y_L is formed in terms of the gyro frequency. From the dipole field, the magnetic field, B at a point in the ionosphere is proportional to the ratio of the cube of the earth's radius to the cube of the distance from the centre of the earth to a point in the ionosphere

$$B \propto \frac{r_0{}^3}{r^3};$$

$$B = \frac{B_0 r_0{}^3}{r^3} \qquad 22$$

r_0 = Earth radius ≈ 6400 km

$$r = r_0 + h \qquad 23$$

h = point in the ionosphere = 220km (base at sunset)

B_0 = equatorial magnetic field = $0.32 \times 10^{-4} T$

$$B = \frac{0.32\times10^{-4}\times(6400)^3}{(6400+220)^3} = 0.29\times10^{-4}T$$

Gyro frequency $\omega_G = 2\pi f_G$

$$f_G = \frac{\omega_G}{2\pi};$$

$$\omega_G = \frac{eB}{m} \qquad 24$$

$$f_G = \frac{1}{2\pi}\frac{eB}{m} = \frac{1.602\times10^{-19}\times0.29\times10^{-4}}{2\times3.142\times9.11\times10^{-31}} = 0.82\times10^6 Hz = 0.8Mhz$$

In the equatorial region, f_G = 0.8Mhz. $\omega^2{}_N = (2\pi f_N)^2 = \frac{Ne^2}{m\varepsilon_0}$ but at reflection point with N_m, f_N = f = 4.9 Mhz where X = 1.

The height, h between the base of the ionosphere at sunset and the maximum height of reflection h_m is y. The maximum of y (y_m) defines the semi thickness of the layer

$$y = h_m - h \qquad 25$$

The electron density, N is

$N = N_m(1 - \frac{y^2}{{y_m}^2})$ 26

$$N_m = 1.24 \times \frac{10^9 e}{m^3} \ (at\ 4.9MHz)$$

The reduced electron density, $X = \frac{Ne^2}{m\varepsilon_0\omega^2}$

$$X = 3.357394 \times 10^{-12}\ N \quad 27$$

for $e = 1.602 \times 10^{-19}C; m = 9.11 \times 10^{-31}kg;\ \varepsilon_0 = 8.85 \times 10^{-12}\ H/m;\ \omega = 2\pi f$

II. Method And Results:

The refractive index $\mu = \left(1 - \frac{X}{1+Y_L}\right)^{1/2}\ for\ Q_L$ but $\mu = (1-X)^{1/2}\ for\ Q_T$

$Z = \frac{\nu}{\omega}$ calculated using $\nu - h$ data (Banks, P. M. et al (1973)).

for $\omega = 2\pi(4.9MHz)$

at reflection point, $X = \frac{{\omega^2}_N}{\omega^2}$; at point of reflection,$\omega_N = \omega$

$L_1 = \int Kds = R\int \frac{N\nu}{\mu} dh$ for $\mu \to 1$ 28

$L_2 = \int Kds = R\int \frac{N\nu}{\mu} dh$ for $\mu \to 0$ 29

$K = \frac{e^2}{2mc\,\varepsilon_0}\frac{1}{\mu}\frac{N\nu}{\nu^2+(\omega\pm\omega_L)^2} = \frac{(1.602\times10^{-19})^2}{2\times9.11\times10^{-31}\times3.0\times10^8\times8.85\times10^{-12}} \cdot \frac{N\nu}{\nu^2+4\pi^2(4.9Mhz+0.8Mhz)^2} = \frac{5.3\times10^{-6}N\nu}{\nu^2+4\pi^2(4.9Mhz+0.8Mhz)^2}$ 30

$R = \frac{e^2}{2mc\,\varepsilon_0}\frac{1}{\nu^2+(\omega\pm\omega_L)^2} = \frac{(1.602\times10^{-19})^2}{2\times9.11\times10^{-31}\times3.0\times10^8\times8.85\times10^{-12}} \cdot \frac{1}{\nu^2+4\pi^2(4.9Mhz+0.8Mhz)^2} = \frac{5.3\times10^{-6}}{\nu^2+4\pi^2(4.9Mhz+0.8Mhz)^2}$ 31

$L_1 = \int Kds = \frac{5.3\times10^{-6}}{\nu^2+(1283\,Mhz)^2}\int \frac{N\nu}{\mu} dh$ for $\mu \to 1$

$L_2 = \int Kds = \frac{5.3\times10^{-6}}{\nu^2+(1283\,Mhz)^2}\int \frac{N\nu}{\mu} dh$ for $\mu \to 0$

Trapezoidal Rule Integration is applied. For this work, the step size in the non-derivative region is 5km and reduces to 1km, 0.1km, 0.01km, 0.001km, 0.0001km and 0.00001km in the absorbing region where deviative absorption takes place Within this range of heights, the integration steps are further reduced. Practically, when $y_m = 130km$, the step size is 5km down to when y=5km. so between 130km and 5km i.e. y_m and y. N can be calculated using;

$N = N_m(1 - \frac{y^2}{{y_m}^2})$; $h = 345\ km$

In this region of the atmosphere, there is non-deviative absorption, where $\mu \to 1$and Nν is large.

$K = 5.9 \times 10^{-16}\frac{N}{\nu} = 4.92 \times 10^{-24}N$ 32

Table1 Summary of the absorption coefficients variation with height, H (km)

Height, h(km)	ν (Hz)	Square of ν	Square of ω	N par/cm^3	Coeff, K/km
50	1.2E+08	1.44E+16	9.48E+14	2.14E+22	0.105042
55	64000000	4.1E+15	9.48E+14	1.18E+22	0.058105
60	34000000	1.16E+15	9.48E+14	6.44E+21	0.031675
65	17000000	2.89E+14	9.48E+14	3.39E+21	0.016696
70	7800000	6.08E+13	9.48E+14	1.72E+22	0.084732
75	3600000	1.3E+13	9.48E+14	8.3E+20	0.004084
80	1500000	2.25E+12	9.48E+14	3.83E+20	0.001886
85	660000	4.36E+11	9.48E+14	1.71E+20	0.000841
90	459000	2.11E+11	9.48E+14	7.12E+19	0.00035
95	193000	3.72E+10	9.48E+14	2.92E+19	0.000144
100	84400	7.12E+09	9.48E+14	1.19E+19	5.85E-05
105	35800	1.28E+09	9.48E+14	5.02E+18	2.47E-05
110	15500	2.4E+08	9.48E+14	2.14E+18	1.05E-05

115	7420	55056400	9.48E+14	9.68E+17	4.76E-06
120	4410	19448100	9.48E+14	5.11E+17	2.51E-06
125	2990	8940100	9.48E+14	3.01E+17	1.48E-06
130	2220	4928400	9.48E+14	1.93E+17	9.5E-07
135	1810	3276100	9.48E+14	1.31E+17	6.46E-07
140	1530	2340900	9.48E+14	9.32E+16	4.59E-07
145	1370	1876900	9.48E+14	6.86E+16	3.37E-07
150	1300	1690000	9.48E+14	5.19E+16	2.55E-07
155	1220	1488400	9.48E+14	4.01E+16	1.97E-07
160	1330	1768900	9.48E+14	3.16E+16	1.56E-07
165	1070	1144900	9.48E+14	2.53E+16	1.25E-07
170	996	992016	9.48E+14	2.06E+16	1.01E-07
175	950	902500	9.48E+14	1.69E+16	8.3E-08
180	890	792100	9.48E+14	1.4E+16	6.89E-08
185	810	656100	9.48E+14	1.17E+16	5.77E-08
190	750	562500	9.48E+14	9.89E+15	4.86E-08
195	690	476100	9.48E+14	8.4E+15	4.13E-08
200	620	384400	9.48E+14	7.18E+15	3.53E-08
205	580	336400	9.48E+14	6.18E+15	3.04E-08
210	490	240100	9.48E+14	5.34E+15	2.63E-08
215	440	193600	9.48E+14	4.63E+15	2.28E-08
220	400	160000	9.48E+14	4.04E+15	1.99E-08
225	390	152100	9.48E+14	3.54E+15	1.74E-08
230	390	152100	9.48E+14	3.11E+15	1.53E-08
235	380	144400	9.48E+14	2.74E+15	1.35E-08
240	380	144400	9.48E+14	2.42E+15	1.19E-08
245	380	144400	9.48E+14	2.15E+15	1.06E-08
250	380	144400	9.48E+14	1.91E+15	9.38E-09
255	390	152100	9.48E+14	1.7E+15	8.35E-09
260	400	160000	9.48E+14	1.52E+15	7.45E-09
265	410	168100	9.48E+14	1.36E+15	6.67E-09
270	430	184900	9.48E+14	1.22E+15	5.98E-09
275	440	193600	9.48E+14	1.09E+15	5.36E-09
280	460	211600	9.48E+14	9.81E+14	4.83E-09
285	470	220900	9.48E+14	8.83E+14	4.35E-09
290	480	230400	9.48E+14	7.97E+14	3.92E-09
295	490	240100	9.48E+14	7.2E+14	3.54E-09
300	500	250000	9.48E+14	6.51E+14	3.2E-09
305	510	260100	9.48E+14	5.78E+14	2.84E-09
310	530	280900	9.48E+14	5.34E+14	2.63E-09
315	540	291600	9.48E+14	4.76E+14	2.34E-09
320	560	313600	9.48E+14	4.41E+14	2.17E-09
325	560	313600	9.48E+14	3.93E+14	1.93E-09
330	570	324900	9.48E+14	3.65E+14	1.79E-09
335	570	324900	9.48E+14	3.26E+14	1.6E-09
340	580	336400	9.48E+14	3.03E+14	1.49E-09

345	590	348100	9.48E+14	2.72E+14	1.34E-09
350	590	348100	9.48E+14	2.52E+14	1.24E-09

Step size of 1km from $y = 5\ km\ to\ 1\ km\ (h = 349\ km)$, Step size of 0.1km from $y = 1\ km\ to\ 0.1\ km$, Step size of 0.01km from $y = 0.1\ km\ to\ 0.01\ km, etc.$

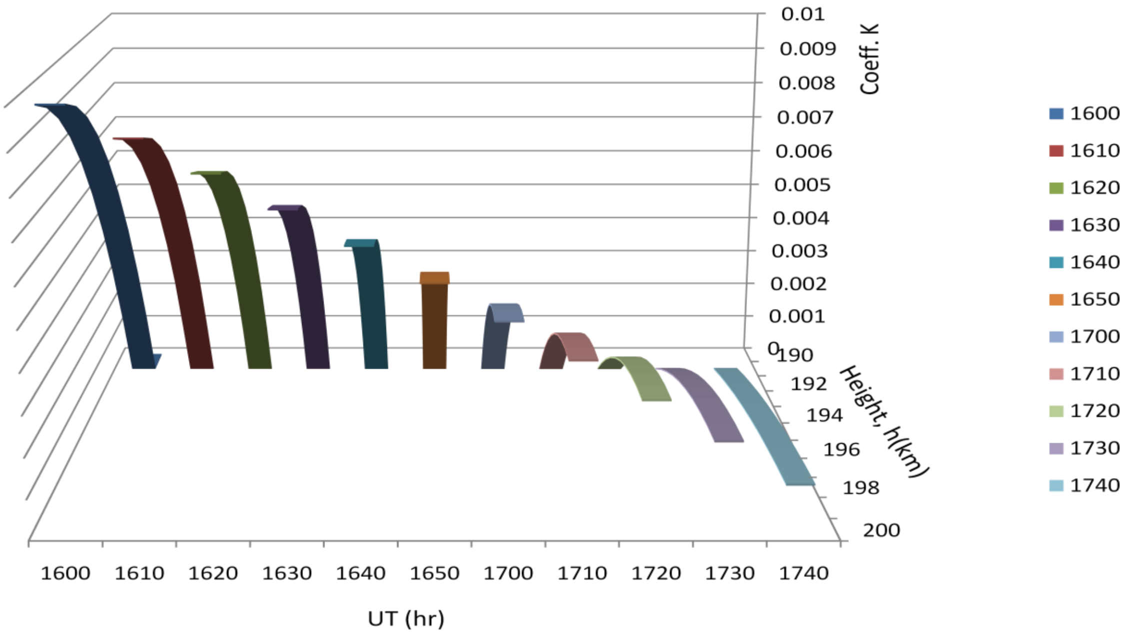

Figure 1 Absorption coefficients determined during early sunset sampled at 1km interval between height of 191 and 200km on 13/12/1980.

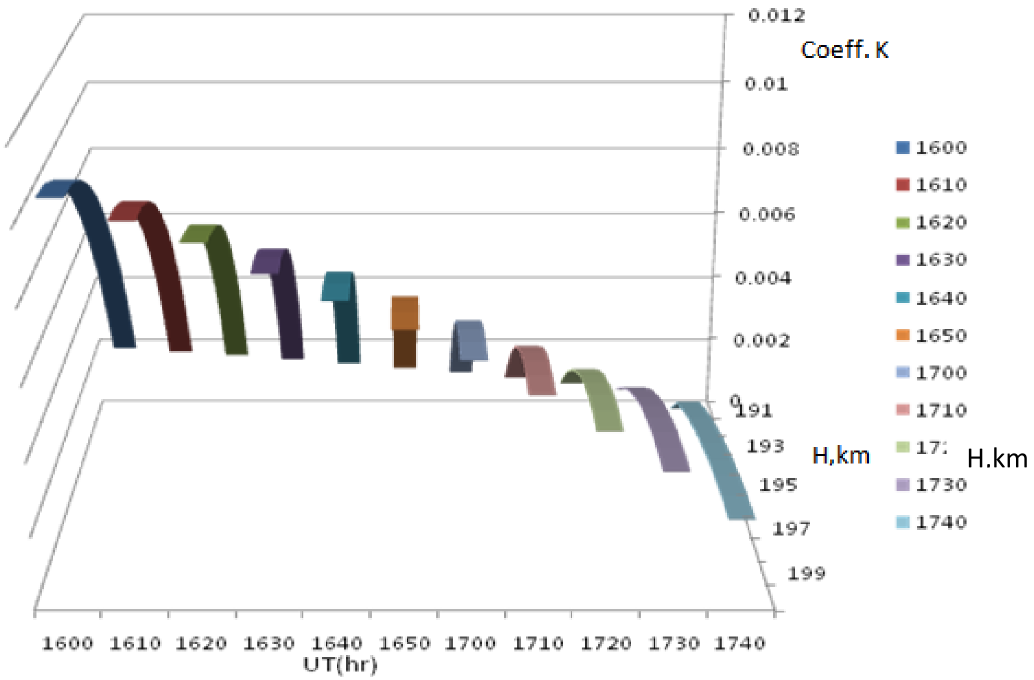

Figure 2 Absorption coefficients determined during early sunset sampled at 1km interval between height of 191 and 200km on 10/01/1981.

III. Analysis and discussion

The absorption coefficient depends on the electron density, N. At 50km, the collision frequency, ν is 1.2×10^8 Hz. This value is much greater than the signal angular frequency ω, which is 5.7 x 10^6 Hz ($\nu^2 \gg \omega^2$).

For other heights and collision frequencies subject to non-deviative absorption, where $\nu^2 \gg \omega^2$ which covers heights below 50 km, $K = 5.9 \times 10^{-16} \frac{N}{\nu}$ can be used. Below 60km, $\nu^2 \gg \omega^2$. Between 65 - 85km, $\nu^2 \cong \omega^2$. From 85km, $\nu^2 \ll \omega^2$. At height of 135km, the electron-neutral collision frequency, $\nu_{en} = 1030Hz$ while the electron-ion collision frequency, $\nu_{ei} = 777Hz$. At the height of 140km, $\nu_{en} = 746Hz$ while $\nu_{ei} = 787Hz$. At the height of 145km, $\nu_{en} = 562Hz$ while $\nu_{ei} = 808Hz$. The electron-ion collision frequency ν_{ei} increases while the electron-neutral collision frequency decreases with height. The increase in the total collision frequency, ν seen from 255km is due to the increase electron- ion collision frequency, ν_{ei}. During sunset, the base of the ionosphere moves to 220km. For signal frequency of 4.9 MHz, the reflection of the signal takes place the height of 350km. The absorption coefficients within these heights range is given in table 1 above. When the refractive index approaches zero ($\mu \to 0$), the absorption coefficient, K is characterized by the electron-ion collision that exhibits an almost constant values. From figure 1 above, the absorption coefficients determined during sunset for one (1) km interval between 191km and 200km show adecrease in absorption with increase in height and as the sunset time moves toward night.

IV. Conclusion

The absorption coefficients for signal of 4.9MHz transmitted from Cotonou to Lagos show decrease as the height increases. This decrease also shows a corresponding relationship with the universal time (UT) as sunset time approaches night time. The sampled data taken during the early sunset period on 13/12/1980 and 10/01/1981show that the absorption coefficient, which is proportional to the particle density, N and collision frequency, ν is due to the electron-ion collision frequency. The electron-neutral collision frequency decreases with height rapidly but the electron-ion increases with height to about 185km and then starts decreasing slowly from the height of 190km leading to the decrease in the absorption coefficients. Quasi longitudinal propagation is largely responsible for the non-deviative absorption. Within the region of non-deviative absorption, the product the electron density, N and the collision frequency ν is large. The deviative absorption is attributed to the refractive index μ that approaches zero ($\mu \to 0$). These values of refractive index are mainly obtained near reflection zone, the signal frequency f is equal to the plasma frequency f_N ($f = f_N$). The wave slows down within this region. Since both electron-neutral and the electron-ion collision frequencies decrease towards the deviative absorption region, the angular signal frequency in equation 30 becomes much greater than the total collision frequency $\omega \gg \nu$. The graph of N against K is more of a moving average and less of a logarithmic one in Figures 1 and 2.

References

[1]. Nathaniel, E. U., Thomas, J. E. and Akpan, S. S. Analysis of the sunset equatorial ionosphere using absorption data. J. of Applied Sciences, Vol. 6, No. 7, ISSN: 2455-6653, 2020.

[2]. Shamsi, (1984). Oblique incidence ionospheric absorption near magnetic equator. University of Lagos Press. Lagos.

[3]. Belova, E. G., Pashin, A. B. a Lyatsky, W. B. Passage of a powerful HF radio wave through the lower ionosphere as a function of initial electron density profiles. J. of Atmos. and Terr. Phys.1995; 37: 265-272.

[4]. Mishin, E. V. and Atamaniuk, B. Radio wave turbulent absorption due to electron injection in the ionosphere. J. of Atmos. and Terr. Phys. 1995; 57: 193-199.

[5]. Rawer, K. Manual on Ionospheric absorption measurements. J. of Atmos. and Terr. Phys. 25. 1967.

[6]. Rawer, K. Wave propagation in the ionosphere; Developments in Electromagnetic theory and applications. Kluwer Academic Publishers. Vol. 5.1993.

[7]. Kelso, J. M. The calculation of ionospheric electron density distributions. J. of Atmos. and Terr. Phys., 1950; 10: 103-109.

[8]. Kelso, J. M. A procedure for the determination of the vertical distribution of the electron in the ionosphere. J. Geophy. Res., 1952; 57: 357-367.

[9]. Titheridge, J. E. Continuous records of the total electron content of the ionosphere. J. of Atmos. and Terr. Phys. 1966; 28: 1135-1150.

[10]. Baumjohann, W. and Treumann, R. A. Basic space Plasma Physics. Imperial College Press, London, 1996.

[11]. Kivelson, M. G. and Russell, C. T. Introduction to Space Physics. Cambridge University Press, 1995.

[12]. Parks, G. K. Physics of Space Plasmas: An introduction. Addison-Wesley Publishing Company, The Advanced Book Program, 350 Bridge Parkway, Redwood City, CA 94065, 1991.

[13]. Folkestad, K. Ionospheric radio communication. Plenum Press, New York, 1968.

[14]. Nielsen, E., Morgan, D. D., Kirchner, D. L., Plaut, J. and Picardi, G. Absorption and reflection of radio wave in the Martian ionosphere. Planetary and space science. 2007; 55: 864-870.

[15]. Banks, P. M. and Kockarts, G. Aeronomy, Part A. Academic Press Inc. LCCC, 1973.

[16]. Unal, I., Ozcan, O. and Canyilmaz, M. Ionospheric absorption of HF radio wave in vertical propagation. Iranian journal of science. Transaction A, 2007; 31(4).

[17]. Zabotin N. A., Bratsun, D. S., Pulinets, S. A. and Benson, R. F. Response of radio sounding signals to small scale field-aligned ionospheric irregularities. J. of Atmos. & Terr. Phys., 59, (17), 2231, (1997).

[18]. Olatunji, E. O. The total columnar electron content of the equatorial ionosphere. J. of Atmos. & Terr. Phys., Vol. 29 pp. 277-285, (1966),

[19]. King, J. W., Olatunji, E. O., Eccles, D. and Newman, W. S. Integrated electron content in equatorial ionosphere. J. of Atmos. & Terr. Phys., Vol. 29 pp. 1391-1396, (1967)

[20]. Thrane, E. V. and Piggot, W. R.. The electron densities in the E and D regions above Kjeller. J. of Atmos. and Terr. Phys. 1966; 28: 467-479.
[21]. Thrane, E. V. Information on the D and E region electron density profiles. Radio Science. 1972; 7(1): 143-145.
[22]. Victor U. Chukwuma (1999). An A3 investigation of the effect of geomagnetic activity on radio wave absorption in the equatorial region. Indian Journal of Radio & Space Physics Vol.28 , December 1999, pp.264-270.

Ekong U. Nathaniel. "Determination of Absorption Coefficients from Qt and Ql Propagation of Signal Frequency in Equatorial Ionosphere At Sunset." *IOSR Journal of Applied Physics (IOSR-JAP)*, 12(4), 2020, pp. 50-57.